Vol. 80: 243–256, 2017
https://doi.org/10.3354/ame01852

AQUATIC MICROBIAL ECOLOGY
Aquat Microb Ecol

Published online December 13

A comparison of bacterial community structure, activity and microcystins associated with formation and breakdown of a cyanobacterial scum

Konstanze Steiner[1,2,*], Susanna A. Wood[1,3], Jonathan Puddick[1], Ian Hawes[3], Daniel R. Dietrich[2], David P. Hamilton[3,4]

[1]Cawthron Institute, Private Bag 2, Nelson 7010, New Zealand
[2]Human and Environmental Toxicology, University of Constance, PO Box 662, 78457 Constance, Germany
[3]Environmental Research Institute, University of Waikato, Private Bag 3105, Hamilton 3240, New Zealand
[4]*Present address:* Australian Rivers Institute Level 4, Sir Samuel Griffith Centre, 170 Kessels Road, Nathan, Queensland 4111, Australia

ABSTRACT: Toxic *Cyanobacteria*-dominated blooms are a global phenomenon that poses a health risk to humans and animals. These blooms harbor a diverse range of heterotrophic bacteria which are involved in growth-promoting and decomposition processes. In the present study, we investigated microbial communities and microcystins in a lake cyanobacterial scum at a single point in time. The outer edges of the scum (ca. 500 cm from shore) were freshly formed, while those closest to the shore showed signs of cyanobacterial cell lysis and degradation. Samples were collected from 5 sites across the scum and from 2 separate bays. We hypothesized that cyanobacterial genera, bacterial communities and microcystin quota (toxin content per cell) would be significantly different in the degrading scums versus where the scum had freshly formed. Samples were analyzed using 16S rRNA metabarcoding (DNA and RNA), and a range of physicochemical parameters were determined. *Microcystis* transcripts were more abundant than *Dolichospermum* in the breaking-down scum, suggesting they are better suited to tolerating the harsh physicochemical conditions encountered within scums. Multivariate analysis of operational taxonomic units (excluding *Cyanobacteria*) showed significant differences in bacterial community structures across the scums. *Proteobacteria* was the most abundant phylum, among which *Aeromonas*, *Caulobacter* and *Brevundimonas* dominated. No relationships were observed between microcystin quotas and bacterial community structure or position in the scum.

KEY WORDS: 16S rRNA gene sequences · *Cyanobacteria* · *Dolichospermum* · High-throughput sequencing · Microbial community · *Microcystis*

INTRODUCTION

Cyanobacteria are found worldwide in diverse environments including oceans, freshwater, bare rock and soil (Whitton 2012). They are particularly problematic in eutrophic freshwater bodies where they can rapidly proliferate, forming surface or sub-surface blooms (Paerl 1988, Oliver et al. 2012, Paerl & Otten 2013). Cyanobacterial blooms can result in reduction of water quality, including oxygen depletion, production of toxic byproducts (methane, hydrogen sulfide and ammonia) and reduced water clarity with restricted light penetration. These changes can have severe consequences for aquatic animals and submerged plants, adversely affecting the sustainability of aquatic ecosystems and food web dynamics (Robarts et al. 2005, Havens 2008, Turner & Chislock 2010). Continued eutrophication and global climate change are predicted to result in an increase in the frequency and intensity of blooms

*Corresponding author: konstanze.steiner@uni-konstanz.de

(Bartram et al. 1999, Paul 2008, Beardall et al. 2009, Paerl & Huisman 2009, Carey et al. 2012, Wood et al. 2017a). Globally, one of the most common bloom-forming cyanobacterial genera is *Microcystis*, with blooms reported in 108 countries (Harke et al. 2016). *Microcystis* strains commonly produce multiple structural forms of toxic microcystins; thus, these blooms pose a health risk for humans and animals, compromise surface waters used for human drinking water supplies, and limit recreational use of affected water bodies (Hitzfeld et al. 2000, Carmichael 2001, Paerl et al. 2001, Kouzminov et al. 2007, Funari & Testai 2008, Stewart et al. 2008).

To improve knowledge of cyanobacterial dominance in phytoplankton communities, research has primarily focused on the influence of physical and chemical factors (Oliver et al. 2012). *Cyanobacteria* co-exist with heterotrophic bacteria; thus, insights into the composition and functioning of these microbial communities might be crucial to understanding the mechanisms leading to bloom formation and senescence (Worm & Sondergaard 1998, Casamatta & Wickstrom 2000, Eiler & Bertilsson 2004, Kolmonen et al. 2004). The region surrounding cyanobacterial cells which acts as a niche for bacteria is known as the phycosphere, analogous to the rhizosphere. Within the phycosphere, bacteria can live freely around the cells, attached to cell surfaces or within their excreted products (Jasti et al. 2005). Organic compounds, such as polysaccharides, excreted by algae provide an energy source for the heterotrophic bacteria, while the bacteria can act as a symbiotic partner by providing carbon dioxide, nitrogen, phosphorus, sulfur and trace elements to their algal hosts (Worm & Sondergaard 1998, Salomon et al. 2003, Havens 2008). The phycosphere of colony-building *Cyanobacteria* like *Microcystis* provides a potential niche for heterotrophic bacteria as they may benefit from the mucilage surrounding the colonies (Worm & Sondergaard 1998, Brunberg 1999). Consequently, the concentrations of heterotrophic bacteria in the mucilage are higher than in the immediate surrounding water (Worm & Sondergaard 1998). Substances excreted by *Microcystis* cells become entrapped in this zone due to the high content of high molecular weight polysaccharides, which causes the mucilage to have high viscosity (Amemiya et al. 1990, Pereira et al. 2009).

Recent studies have highlighted the influence of heterotrophic bacteria on cyanobacterial growth, colony formation and bloom decline (Manage et al. 2000, Rashidan & Bird 2001, Berg et al. 2009, Shen et al. 2011, Cai et al. 2014, Wang et al. 2015). Some bacteria enhance growth, while others exhibit an inhibitory effect or may even terminate blooms through excretion of algicidal substances (Manage et al. 2000, Rashidan & Bird 2001, Berg et al. 2009). Bacterial community composition can differ depending on *Microcystis* colony size and can change during breakdown of colonies, accompanied by alterations in extracellular compound composition, suggesting an interaction between heterotrophic bacteria, mucilage composition and colony aggregation (Shen et al. 2011, Cai et al. 2014, Wang et al. 2015).

In the present study, a cyanobacterial scum (ca. 500 cm wide) had formed naturally along the shoreline of a small eutrophic lake over a period of approximately 3 d. The outer edges of the scum were freshly formed, while those closest to the shore showed signs of cyanobacterial cell lysis (see Fig. 1B,C). This provided a unique opportunity to investigate shifts in bacterial communities associated with a cyanobacterial scum in varying states of viability at a single point in time. We hypothesized that (1) *Cyanobacteria* genera would show different abilities to survive the various stages of scum formation and breakdown, (2) there would be significant shifts in the active heterotrophic bacteria associated with the cyanobacterial phycosphere across the scum formation and breakdown gradient, and (3) the bacterial community composition or the presence of certain heterotrophic bacteria would influence microcystin quota (amount of toxin per cell). Improved knowledge of the role of heterotrophic bacteria in the phycosphere may ultimately assist in understanding factors that regulate cyanobacterial bloom formation and senescence.

MATERIALS AND METHODS

Study site and sample collection

Lake Waitawa is a small (ca. 16 ha) shallow (<7 m max. depth) eutrophic lake northeast of Wellington, New Zealand (our Fig. 1; Perrie & Milne 2012). Sampling was undertaken on 5 May 2015 with minimal temporal variability (between 09:00 and 11:00 h). A cyanobacterial scum (defined as a visible surface accumulation of *Cyanobacteria* colonies) had accumulated along the lake shore and extended out into the lake a distance of 500 cm. Close to shore (within ~100 cm), the scum had remained stagnant for several days and started to break down. This was visible as an intense blue coloration of the scum, indicating phycocyanin release after cell lysis. With increasing

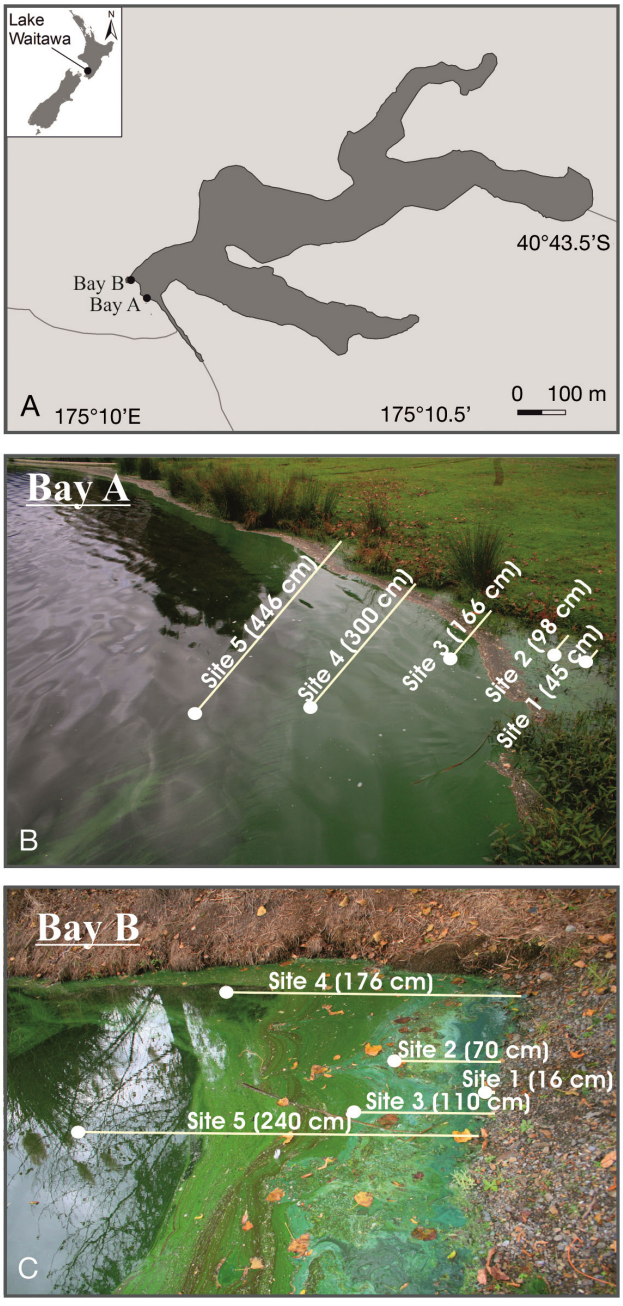

Fig. 1. (A) Lake Waitawa and sampling sites (inset: New Zealand). Location and distance from shore of samples taken from 5 sites at (B) Bay A and (C) Bay B

distance from shore, the coloration of the scum changed gradually from blue to green (Fig. 1B,C). This scum formation was observed in 2 different downwind bays (Bay A and Bay B; Fig. 1A). The selected bays were only approximately 100 m apart, and were orientated in the same direction. From each bay, 5 samples (50 ml) were collected from sites with increasing distance from the shore (16–446 cm). The samples were either collected from parts of the scums showing signs of breakdown (Bay A: Sites 1 and 2, and Bay B: Sites 1 and 2) or scums that had freshly formed (Bay A: Sites 3–5, and Bay B: Sites 3–5; Fig. 1B,C).

Subsamples for *Microcystis* and *Dolichospermum* enumeration (1 ml) were preserved with Lugol's iodine. Subsamples for molecular analysis were filtered (GF/C, pore size ca. 1.2 µm, Whatman; volumes between 1 and 27 ml depending on the scum density), and the filter was stored in LifeGuard Preservation Solution (MoBio Laboratories) at −20°C for subsequent DNA and RNA extraction. These filters would allow most free-living bacteria to pass through them, but capture *Cyanobacteria* cells and associated bacteria in the phycosphere. Subsamples for total microcystin analysis (1 ml) and total nutrient analysis (5 ml) were frozen (−20°C). The remaining sample was pre-filtered (50 µm mesh), filtered (GF/C, Whatman), and aliquots of the filtrate taken for analysis of extracellular microcystins (1 ml; stored at −20°C) and dissolved nutrients (5 ml; stored at −20°C). At each sampling site, temperature, dissolved oxygen (DO), pH, chlorophyll *a* (chl *a*) and phycocyanin (combined measurement for intra- and extracellular concentrations) were measured (EXO2 water quality sonde, YSI).

Microcystis and *Dolichospermum* enumeration

Lugol's iodine-preserved samples were mechanically ground (Wheaton Tissue Grinder) with 50 strokes to disaggregate colonies as described in Wood et al. (2017a). Diluted subsamples were allowed to settle in 12-well plates (Thermo Scientific) for 3 h. *Microcystis* and *Dolichospermum* cells within 10 random fields were counted at 400× magnification using an inverted microscope (CKX41, Olympus).

DNA and RNA extraction and cDNA synthesis

To discriminate between active and dormant or dead bacteria in the samples, 16S rRNA metabarcoding using high-throughput sequencing (HTS) was performed on DNA and RNA. DNA and RNA were co-extracted from filters using the ZR-Duet™ DNA/RNA MiniPrep Kit (Zymo Research) according to the manufacturer's protocol. The quality and purity of isolated RNA and DNA were checked on 1.5% agarose gels and using a Nanophotometer (Implen). Trace DNA molecules carried over in RNA extracts

were eliminated by 2 sequential DNase treatments as in Langlet et al. (2013). The efficiency of the DNase treatment was verified by running a PCR using the reagents and conditions used for the down-stream 16S rRNA amplification (see next subsection). Extracted RNA was reverse-transcribed using SuperScript® IV reverse transcriptase (Life Technologies). The various extract products (DNA, cDNA and RNA) were separated into aliquots and stored frozen (–20°C for DNA and –80°C for RNA) until further analysis.

HTS

A region of the 16S rRNA gene ca. 400 bp long was amplified using bacterial-specific primers (IlumF-Bakt_341 and IlumR-Bakt_805R, Table S1 in the Supplement at www.int-res.com/articles/suppl/a080p243_supp.pdf) modified to include Ilumina™ adapters.

PCR reactions were performed in 50 µl volumes containing 25 µl of AmpliTaq Gold® 360 master mix (Life Technologies), 12.5 µl CG inhibitor (Life Technologies), 2 µl of each primer (10 µM, Integrated DNA Technologies), 2 µl template DNA or cDNA (between 60 and 220 ng) and 6.5 µl Milli-Q water. PCR cycling conditions were 95°C for 10 min, followed by 27 cycles of 95°C for 30 s, 50°C for 30 s, 72°C for 45 s, and a final extension of 72°C for 7 min. PCR products were visualized with 1.5% agarose gel electrophoresis with Red Safe DNA Loading Dye (iNtRON Biotechnology) and UV illumination to ensure amplification of a single 400 bp product. PCR products were purified (Agencourt® AMPure® XP Kit, Beckman Coulter), quantified (Qubit® 20 Fluorometer, Invitrogen), diluted to 10 ng μl^{-1} and submitted to New Zealand Genomics (Auckland) for library preparation. Sequencing adapters and sample-specific indices were added to each amplicon via a second round of PCR using the Nextera™ Index kit (Illumina™). Amplicons were pooled into a single library and paired-end sequences (2 × 250) were generated on a MiSeq instrument using the TruSeq™ SBS kit (Illumina™). Sequence data were automatically demultiplexed using MiSeq Reporter (v.2), and forward and reverse reads were assigned to samples.

Bioinformatic analysis of metabarcoding data was performed using VSEARCH (Edgar 2010, Flouri et al. 2015). All sequence reads were assessed for quality, and any read that contained a base where the reported Phred quality score dropped below 30 was discarded. Forward and reverse paired-end sequences were assembled independently for each sample using VSEARCH. Merged reads that were <200 bp in length were discarded. The data was then filtered with VSEARCH, discarding all reads that had >1 error per assembled read (Edgar & Flyvbjerg 2015). The retained sequences were dereplicated into unique sequences and aligned against the SILVA bacteria reference database (Pruesse et al. 2007). Chimeras were identified and removed from the dataset using the UCHIME algorithm (Edgar et al. 2011) in dataset mode. Operational taxonomic units (OTUs) were generated using VSEARCH by clustering sequence reads at the 97% similarity threshold. Singletons were removed from the dataset. To account for differential sequencing depth among samples, the number of reads per sample (rps) was rarefied (randomly down-sampled to 20 000 rps). The DNA sample from Bay B: Site 2 was excluded from further analysis, since it only contained 5500 reads. The remaining OTUs were taxonomically assigned using the Ribosomal Database Project (RDP) taxonomic database Version 9 (Cole et al. 2014) using the RDP classifier (Wang et al. 2007) implemented in QIIME (Caporaso et al. 2010) with minimum identity value set at 97%. Sequences of unknown, archaeal, or eukaryotic origin were removed.

Detection of potential microcystin-producing strains

The microcystin-producing potential of the cyanobacterial species in the samples was assessed by PCR amplification of a conserved region of the *mcyE* gene (HEP-F and HEP-R, Table S1). We tested 2 DNA samples — in which the cyanobacterial community was dominated by either *Microcystis* (Bay A: Site 2) or *Dolichospermum* (Bay A: Site 4) — as a template for the PCR reaction setup (as described for the HTS reaction). PCR cycling conditions were 94°C for 5 min, followed by 45 cycles of 94°C for 20 s, 50°C for 20 s, 72°C for 45 s, and a final extension of 72°C for 5 min. Visualization of PCR products with 1.5% agarose gel electrophoresis revealed a single product of approximately 470 bp length. Amplicons were purified with the AxyPrep PCR Clean-up Kit (Axygen Biosciences) and sequenced bi-directionally with the BigDye Terminator v.3.1 Cycle Sequencing Kit (Applied Biosystems) using the HEP-F and -R primers (Table S1). The sequences

were compared with the NCBI GenBank database using BlastN (Benson et al. 2008).

Quantitative PCR for *mcyE* enumeration

To calculate microcystin quota, it was necessary to relate intracellular microcystin concentrations to the concentration of toxic *Microcystis* cells in each sample. Using a quantitative PCR (qPCR) assay, the portion of toxic *Microcystis* cells present was determined by amplifying the *mcyE* gene (a single copy gene). The number of *mcyE* genes (and thus toxic *Microcystis* cells) was determined using a standard curve generated with microcystin-producing *Microcystis* sp. strain CAWBG617 (Wood et al. 2017a). A culture of CAWBG61 was grown under a light regime of 90 µmol m^{-2} s^{-1} with a 12 h light:12 h dark cycle, at a temperature of 18 ± 1°C in a glass flask (500 ml) in MLA medium (Bolch & Blackburn 1996). When the culture was in the exponential growth phase, a subsample (15 ml) was filtered onto a GF/C filter (Whatman). A second subsample (10 ml) was preserved in Lugol's iodine and used to determine the cell concentration by light microscopy, as described above under '*Microcystis* and *Dolichospermum* enumeration'.

Prior to *mcyE* enumeration, all samples were screened for inhibition using an internal control qPCR assay. Each 12.5 µl reaction contained 6.25 µl of KAPA Probe Fast qPCR Kit Master Mix 2×, 0.5 µl of primers (10 µM) targeting internal transcribed spacer region 2 of the rRNA gene operon of *Oncorhynchus keta* salmon sperm (SketaF2 and SketaR3, Table S1), 0.2 µl of probe, 1 µl of extracted salmon sperm DNA (SketaP2, 100 µg ml^{-1}; Sigma), 1 µl of DNA sample and 3.05 µl Milli-Q water. The cycling profile was 95°C for 3 min, followed by 50 cycles of 95°C for 3 s and 58°C for 10 s. If inhibition was observed, samples were diluted and re-analyzed.

Determination of copy numbers of *Microcystis mcyE* genes using qPCR was achieved using the following 12.5 µl reaction mix: 6.25 µl of KAPA Probe Fast qPCR Kit Master Mix 2×, 0.5 µl of *mcyE* primers (10 µM, mcyE-F2 and MicmcyE-R8, Table S1) targeting a region within the *mcyE* open reading frame of the microcystin synthase gene, 0.2 µl of *mcyE* primers probe (mcyE-probe, Table S1), 1 µl of DNA and 4.05 µl Milli-Q water. The cycling profile was 95°C for 3 min, followed by 50 cycles of 95°C for 3 s and 58°C for 10 s. DNA from CAWBG617 was used to generate 6-point standard curves ranging from 7.7 × 10^2 to 7.7 × 10^6 cells ml^{-1}. Each point of the standard curve was analyzed in triplicate for each qPCR run conducted. The standard curves generated were linear ($R^2 > 0.99$) and PCR efficiencies were >0.8.

Nutrient and microcystin analysis

Total phosphorus (TP) and dissolved reactive phosphorus (DRP) were analyzed on a Lachat Quick Chem® Flow Injection Analyser (FIA+ 8000 Series, Zellweger Analytics) using methods given in APHA (2005). The limits of detection for both were 0.004 mg l^{-1}. Subsamples collected for total microcystin analysis were freeze-thawed and sonicated (30 min, 60 kHz) 4 times after supplementing with formic acid at a final concentration of 0.1% (v/v). Following centrifugation (10 000 × *g*, 5 min), the supernatant and the subsamples for extracellular microcystin were analyzed using LC-MS/MS as described in Puddick et al. (2016). Microcystin quota was calculated by summing the concentration of all congeners observed, subtracting the extracellular microcystin concentration and dividing by the number of *mcyE* genes per ml (as determined using qPCR).

Statistical analysis

The untransformed metabarcoding data (number of reads per OTUs per sample) were used to generate OTU rarefaction curves for each sample using the vegan package in R software (Oksanen et al. 2013). The HTS sequence data were then 4th-root-transformed and shade plots were used to visually display patterns of change in the relative abundance in cyanobacterial genera for both DNA and RNA, and the top 25 bacterial taxa (excluding *Cyanobacteria*) using RNA data only.

The OTU data were analyzed using non-metric multidimensional scaling (MDS) based on Bray-Curtis similarities using the PRIMER 7 software package (PRIMER-E). Non-metric MDS was undertaken with 100 random restarts and results were plotted in 2 dimensions. Agglomerative, hierarchical clustering of the Bray-Curtis similarities was performed using the CLUSTER method of the PRIMER software, and this information was superimposed onto the 2-dimensional MDS plot at similarity levels of 58%. Based on the observed clustering of sites in the MDS plot, we then used 1-way distance-based permutational analysis (PERMANOVA, Anderson 2001) to determine if there were significant differences in bacterial community structure (OTUs; RNA

only) between sites close to the shore (Bay A: Sites 1–2 and Bay B: Sites 1–2) and sites further away (Bay A: Sites 3–5 and Bay B: Sites 3–5).

RESULTS

Degradation state, abiotic parameters and nutrient concentrations

Temperature and pH did not differ markedly between samples (Table 1). DO decreased in Bay A with distance from shore (from 13 mg l^{-1} at Site 1 to 6.9 mg l^{-1} at Site 5), whereas in Bay B, less variation was observed. DO was highest at Site 3, at 11.6 mg l^{-1}, while all other sites had a DO concentration between 9.4 and 10.5 mg l^{-1}. Sites closer to shore in both bays showed increasingly intense blue coloration (Fig. 1), most likely indicative of extracellular phycocyanin following release from lysis of cyanobacterial cells. Correspondingly, phycocyanin concentrations (combined measurement of intra- and extracellular concentrations) in both bays varied between 108 and 140 µg l^{-1} at Sites 1–3, and decreased to between 0.1 and 23 µg l^{-1} at Sites 4 and 5. Chl *a* concentrations were highest at Site 2 (Bay A: 574 µg l^{-1}, Bay B: 247 µg l^{-1}), followed by Site 1 (Bay A: 248 µg l^{-1}, Bay B: 199 µg l^{-1}), and decreased at Sites 3, 4 and 5 in both bays (Table 1). *Microcystis* cell and TP concentrations decreased with distance from shore and were generally higher in Bay A than Bay B. DRP was highest at Sites 1 and 2 in Bay A, and Sites 1–3 in Bay B (Table 1).

Dominance of cyanobacterial species and their potential to produce microcystin

In both the DNA and RNA analyses, *Microcystis* sequences were more abundant closer to the shore (Sites 1 and 2 of both bays, between 52% and 93% of all cyanobacterial sequences), while *Dolichospermum* was most prevalent in samples furthest from the shore (Sites 3–5 of both bays; Fig. 2A,B, between 69% and 94% of all cyanobacterial sequences). A third *Cyanobacteria* genus, *Woronichinia*, was present in <5% of all cyanobacterial sequences, with the exception of the DNA sample from Bay B: Site 1, where it made up 29%. *Microcystis* RNA sequences obtained from DNA were more prevalent close to the

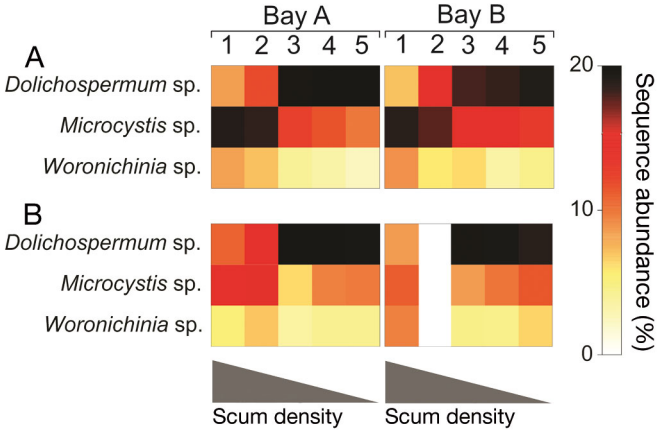

Fig. 2. Heatmap showing percentage abundance of cyanobacterial 16S rRNA reads based on (A) RNA and (B) DNA from Sites 1–5 in Bays A and B. Data are 4th-root-transformed

Table 1. Physicochemical and biological parameters measured at the 5 sites in each bay (Lake Waitawa, 5 May 2015; see Fig. 1B,C)

	Bay A					Bay B				
Site:	1	2	3	4	5	1	2	3	4	5
Physicochemical parameters										
Water temperature (°C)	15.2	15.3	15.1	14.6	14.7	13.1	14.0	14.4	14.6	14.3
Dissolved oxygen (mg l^{-1})	12.96	10.02	8.91	7.96	6.87	9.61	10.48	11.61	10.43	9.43
pH	7.8	7.8	7.6	7.7	7.3	6.9	7.6	7.9	7.6	7.5
Distance to shore (cm)	45	98	166	300	446	16	70	110	176	240
Chl *a* (µg l^{-1})	248	574	114	13	3	199	247	42	17	11
Phycocyanin (µg l^{-1})	142	142	138	15	0.1	140	140	108	23	15
Dissolved reactive phosphorus (mg l^{-1})	0.94	3.13	0.24	0.21	0.14	4.74	2.04	1.57	0.17	0.20
Total phosphorus (mg l^{-1})	49.7	48.3	54.8	2.57	0.3	33.9	43.9	35.7	6.6	0.4
***Microcystis* abundance**										
Total (cells µl^{-1})	30 646	12 643	6532	174	12	5942	7225	5527	1842	77
Toxic genotypes (cells µl^{-1})	1089	194	67	30	0	1501	2157	1516	98	5
***Dolichospermum* concentration**										
Total (cells µl^{-1})	457	7226	19 276	415	3	455	140	13 573	855	19

shore, while the opposite pattern was observed for *Dolichospermum*.

In order to determine the microcystin-producing potential of the *Cyanobacteria* genera present in samples, the *mcyE* genes of 2 samples were sequenced (Bay A: Site 2, a sample where *Microcystis* dominated 84% of all cyanobacterial sequences, and Bay A: Site 4, a sample where *Dolichospermum* dominated 90% of all cyanobacterial sequences). Sequencing results showed that a single *mcyE* amplicon was present, which was 99–100% similar to *mcyE* sequences from cultured *Microcystis* strains (e.g. GenBank accession nos. FJ393327, KF219525, KF219500), and only 76–77% similar to *Dolichospermum flos-aquae* (EU916754) and *Dolichospermum lemmermannii* (EU916752).

Heterotrophic bacterial composition at high taxonomic levels

Rarefaction curves indicated that all samples were adequately sequenced (Fig. S1 in the Supplement at www.int-res.com/articles/suppl/a080p243_supp.pdf). In general, bacterial community composition patterns were similar among DNA and RNA data. We focused on RNA data to ensure that only the functionally active portion of the microbial community was analyzed. When cyanobacterial sequences were excluded, 9 *Bacteria* phyla were identified. The most dominant phyla were *Proteobacteria*, *Bacteroidetes*, *Firmicutes* and *Verrucomicrobia* (Fig. 3). *Proteobacteria* dominated in all samples (80–94%; Fig. 3A). Within this phylum, the most abundant classes were

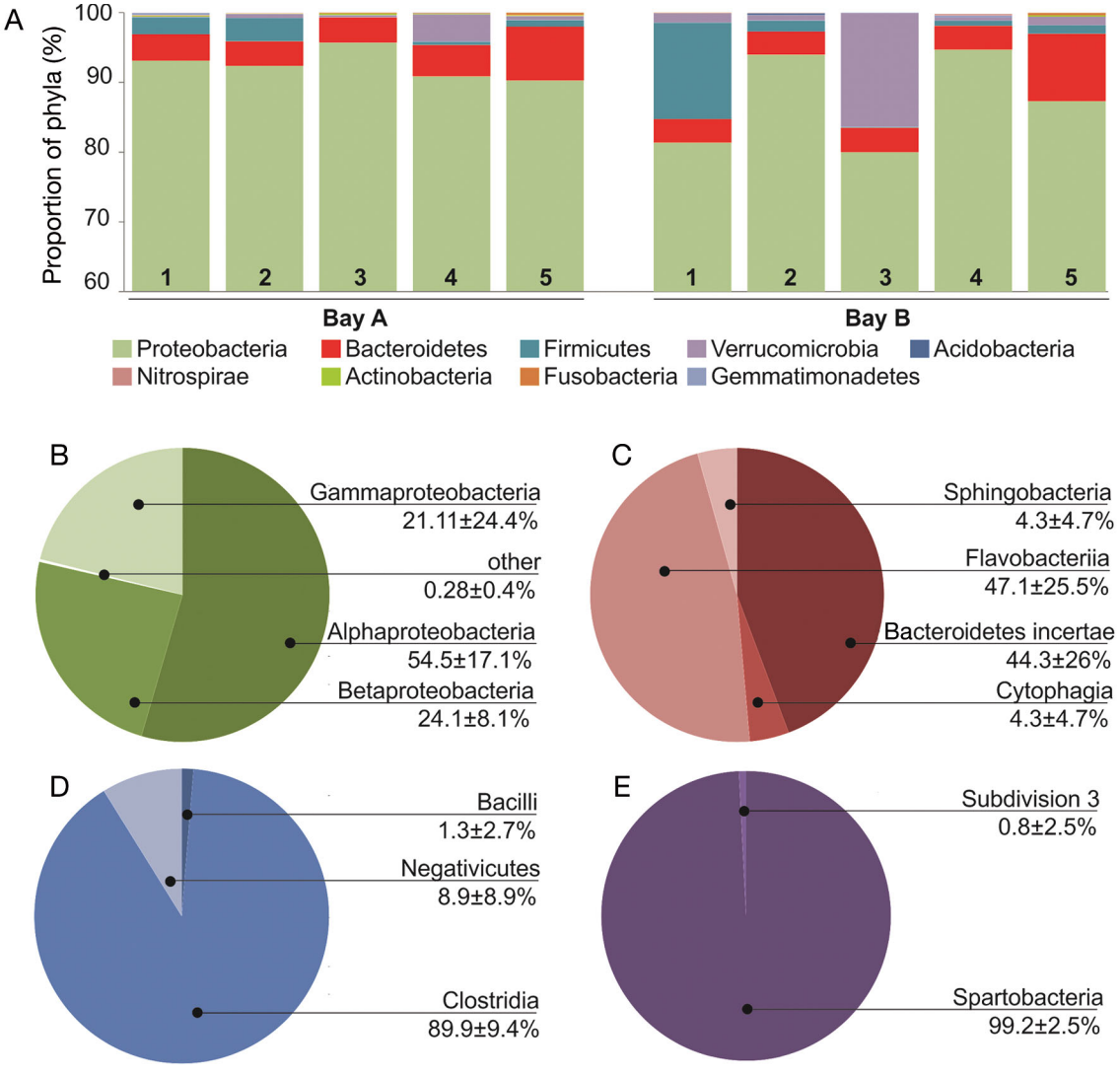

Fig. 3. Relative abundance of heterotrophic bacterial composition (excluding *Cyanobacteria* sequences) at (A) phylum level from Sites 1–5 in Bays A and B. Percentage abundance of class within the phyla (B) *Proteobacteria*, (C) *Bacteroidetes*, (D) *Firmicutes* and (E) *Verrucomicrobia*

Alphaproteobacteria (55%), *Betaproteobacteria* (24%) and *Gammaproteobacteria* (21%; Fig. 3B). There was a notable shift in this pattern in the sample from Bay B: Site 1, where *Gammaproteobacteria* were dominant (82%; data not shown). *Bacteroidetes* was present at low levels in all samples (3.3–9.7%, Fig. 3A), with the most abundant classes being *Flavobacteriia* (47%) and *Bacteroidetes incertae sedis* (44%; Fig. 3C). *Firmicutes* accounted for up to 13.8% (Fig. 3A), with *Clostridia* accounting for 90% of sequences (Fig. 3D), and *Verrucomicrobia* up to 16.3% (Fig. 3A), with *Spartobacteria* accounting for 99% of these sequences (Fig. 3E). *Firmicutes* were generally more abundant at Sites 1 and 2 in both bays (1.6–13.8%) and less abundant at all other sites (<1.2%, Fig. 3A). *Verrucomicrobia* was most abundant at Bay B: Site 3 (16.3%, Fig. 3A), but accounted for <13.9% in all other samples. Other phyla present were *Actinobacteria*, *Fusobacteria*, *Gemmatimonadetes*, *Nitrospirae* and *Acidobacteria*, each accounting for <0.5% of sequences (Fig. 3A).

Comparative bacterial composition at OTU level

To further investigate variations in the active bacterial community composition between samples, 16S rRNA sequences of the 25 most abundant OTUs were analyzed and abundances are shown as a shade plot in Fig. 4. Taxonomy is assigned to the lowest definable level. In general, bacterial abundance of these OTUs was higher at Sites 1 and 2 in both bays compared with the samples from Sites 3–5 in both bays. *Aeromonas* and *Brevundimonas* were more prominent in Sites 1 and 2 of both bays (18% to 36%, respectively), while *Caulobacter* showed a contrasting pattern, dominating in samples from Sites 3–5 of both bays. The next most abundant taxa were *Rhizobiales* and *Comamonadaceae*, accounting for ca. 8% in all samples. Other taxa among the top 25 accounted for <5%. The non-metric MDS ordination showed a clear clustering of the heterotrophic bacteria community into Sites 1 and 2 from both bays, and Sites 3–5 from both bays (Fig. 5), a result which was confirmed as statistically significant using PERMANOVA ($F = 4.395$, $p = 0.004$).

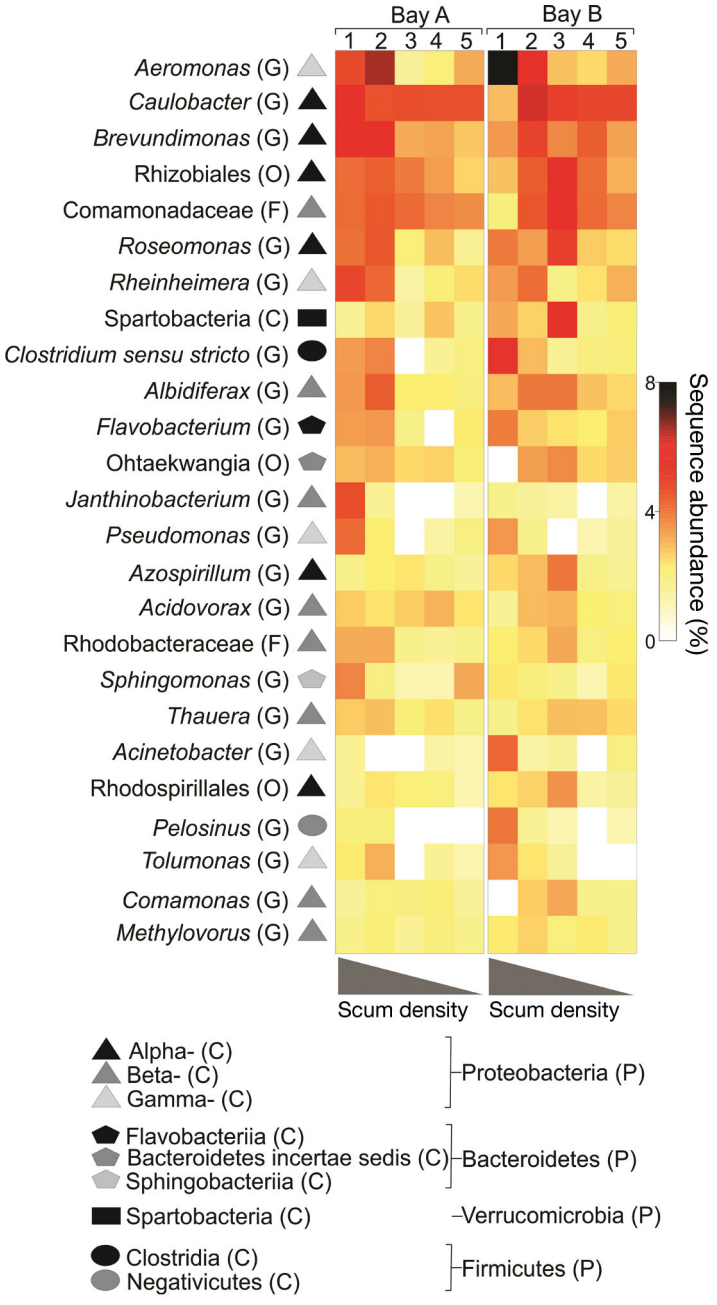

Fig. 4. Heatmap showing abundance of heterotrophic *Bacteria* based on RNA, from Sites 1–5 in Bays A and B. Data are 4th-root-transformed. Data are shown at the lowest taxonomic unit that could be assigned to each operational taxonomic unit (OTU): genus (G), family (F), order (O) or class (C). Symbols adjacent to the OTU indicate the class and phylum (P) they belong to

Microcystin concentrations

In general, changes in the total microcystin concentrations matched the observed shifts in *Microcystis* abundance (as determined by microscopy; Table 1; Fig. S2). The portion of toxic genotypes did not follow the same pattern. In Bay A, it was low (<4%) at Sites 1–3 and 5, and higher at Site 4 (17%). In Bay B, it was relatively consistent among

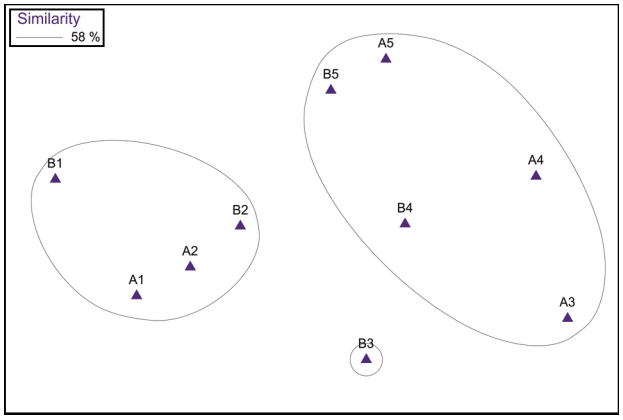

Fig. 5. Two-dimensional non-metric multidimensional scaling ordination (stress = 0.05) based on Bray-Curtis similarities of 16S rRNA sequences (RNA only; 4th-root-transformed) of bacterial communities (excluding *Cyanobacteria*). Points enclosed by line cluster at 58%. A1 to A5 indicate Sites 1 to 5, respectively, in Bay A; B1 to B5 indicate Sites 1 to 5 in Bay B

Sites 1–3 (25–30%), and much lower (<6.5%) at Sites 4 and 5 (Table 1; Fig. S2D). The total microcystin concentration decreased with distance from the shore in Bay A from 2705 ng ml^{-1} (Site 1) to 0.6 ng ml^{-1} (Site 5; Fig. 6A). In Bay B, total microcystin concentrations at all sites were lower than at Sites 1 and 2 in Bay A, and ranged between 182 and 748 ng ml^{-1}. Microcystin quota was highest at Sites 1 and 2 in Bay A and Site 2 in Bay B (Fig. 6B). Microcystin congeners were similar among all samples but different between the intracellular and extracellular fractions (Fig. S2A,B). Intracellular microcystin accounted for the majority of total microcystin (>95% in all samples except for Site 5 in Bay A; Fig. S2C).

DISCUSSION

Changes in bacterial communities during the decline of cyanobacterial blooms have been described over long temporal periods (i.e. months; Shi et al. 2011). Relating these shifts to growth-enhancing or cellular breakdown processes is challenging, as changes in other environmental variables, e.g. temperature and nutrients, may also impact bacterial community composition (Shi et al. 2011, Cai et al. 2014). In the present study, a scum, freshly forming at the outer edge and in the process of breaking down close to the shore, provided a unique opportunity to explore the dominance of cyanobacterial genera during bloom degradation and characterize the bacterial community across the scum with minimal temporal (2 h) and spatial (<500 cm distance) differences. The observed bacterial community structures are a snapshot in time. Physical and chemical parameters at these sites are dynamic and can change on short (i.e. diurnal) time scales, effecting the community composition. Additionally, many bacterial taxa have short doubling times (<24 h) and can respond rapidly to these environmental shifts. In general, both bays showed a similar pattern in cyanobacterial and heterotrophic bacterial community composition, with shifts observed across the scum gradient. There were, however, differences between the bays in microcystin quotas and the presence of specific OTUs, suggesting abiotic parameters other than those measured differed between bays. We anticipated DNA would be present due to recent cell lysis, and therefore, RNA transcripts were also used to prepare our 16S rRNA library to ensure that only the active proportion of the bacterial community was examined. As RNA has limited stability outside the

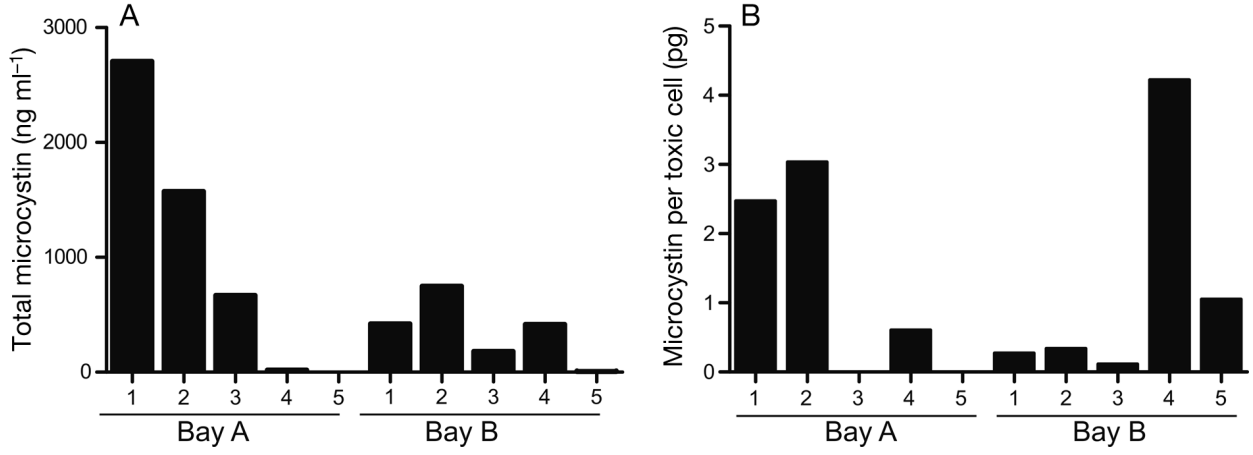

Fig. 6. (A) Total microcystin concentration and (B) microcystin cell quota (concentration per toxic cell), from Sites 1–5 in Bays A and B

cell, this approach ensured that only viable bacteria were assessed (Dell'Anno & Danovaro 2005, Mengoni et al. 2005).

Cyanobacterial composition and viability across the scum

Analysis of the RNA data indicated that viable and active *Microcystis* cells were more abundant than *Dolichospermum* cells in the scum closest to shore which was showing signs of breakdown. Natural lysis of cells can occur due to the breakdown of the cell wall and can be caused by factors such as strong irradiance, contact with other phytoplankton, and parasitism by bacteria or viruses (Fallon & Brock 1979, Shunyu et al. 2006, Pollard & Young 2010, Arii et al. 2015, Spungin et al. 2016). When cyanobacterial cells accumulate on the surface of waterbodies, forming dense scums, photosynthesis can create extreme conditions within a thin layer, including elevated pH, carbon depletion and saturated oxygen levels (Ibelings & Maberly 1998). These conditions, coupled with increased temperature, high irradiance and desiccation stress at the water-air interface create an environment that could promote cell lysis. In the present study, a nearly 2-fold difference in DO was observed in Bay A, aligning with shifts in cyanobacterial densities. In contrast, the pattern was less evident in Bay B, possibly reflecting the complex nature of these communities, which are a mixture of photosynthetic organisms producing oxygen, and heterotrophic taxa consuming oxygen particularly in the decomposing parts of the scum. The dominance of active *Microcystis* cells in samples taken from areas where dense and decaying scums occurred suggests that this genus may be better able to withstand these conditions than *Dolichospermum*. In the natural environment, *Microcystis* is generally present in colonial form. Colony formation has been shown to have a protective effect by reducing photoinhibition (Wu et al. 2011) and desiccation, and the mucilage surrounding the colonies may also contain antibacterial agents (De Philippis & Vincenzini 1998). Additionally, some bacteria associated with *Microcystis* are known to be beneficial (i.e. through the supply of nutrients), and these symbiotic relationships may enhance the survival of this genus in the decaying scums (Brunberg 1999, Salomon et al. 2003, Berg et al. 2009). The ability to withstand the extreme physicochemical conditions that occur during scums may give *Microcystis* a competitive advantage over other cyanobacterial genera and contribute to the prevalence of this bloom-forming taxa worldwide (Harke et al. 2016).

Bacterial composition across the scum

The bacterial communities (excluding cyanobacterial sequences) from Sites 1 and 2 were significantly different from Sites 3–5 in both bays. There are 2 key factors that could be responsible for structuring these communities: (1) the dominance of *Microcystis* or *Dolichospermum*, and (2) the stage of scum degradation. Specific heterotrophic bacteria have been shown to be associated with different *Cyanobacteria* genera, and it has been suggested this is associated with adaptation to specific *Cyanobacteria* metabolites (Louati et al. 2015). Most studies have focused on bacterial communities associated with *Microcystis*, and data from other genera are limited. Louati et al. (2015) demonstrated that bacterial communities differ depending on the dominant cyanobacterial genera (*Microcystis* or *Dolichospermum*) in a study conducted over several months. Our data add further evidence to support their suggestion, as other changes in variables during their study period (e.g. temperature) were not present in our study, as it was conducted at one point in time.

The results of the present study indicate that decomposition state of the scum also influences bacterial communities, with samples from the scum that was decomposing dominated by taxa that are able to break down complex molecules. These results are supported by Parveen et al. (2013), who found that heterotrophic bacteria tend to accumulate around dead *Microcystis* cells, although it is not clear whether these bacteria induced *Microcystis* cell death from algicidal activity, or whether they benefited from the dead cells which provide a source of organic material. Species commonly associated with the recycling of organic matter belong mostly to the phyla *Proteobacteria*, *Bacteroidetes* and *Firmicutes* (Cottrell & Kirchman 2000, Shi et al. 2011, Parveen et al. 2013, Cai et al. 2014). *Proteobacteria* was highly abundant in our samples, making up at least 80% of all non-cyanobacterial sequences. Most of the remaining non-cyanobacterial sequences were identified as *Bacteroidetes*, *Firmicutes* and *Verrucomicrobia* (up to 16%), and have previously been associated with *Microcystis*, although in differing proportions (Shi et al. 2011, Parveen et al. 2013, Cai et al. 2014). Within these phyla, several bacterial phylotypes were present in the top 25 OTUs of our samples,

which are known to either degrade high molecular weight organic matter (e.g. *Clostridium* belonging to the phylum *Firmicutes*) or a range of high to low molecular weight compounds (e.g. *Aeromonas*, *Azospirillum*, *Pseudomonas*, all belonging to the phylum *Proteobacteria*). In the present study, *Aeromonas* (belonging to *Gammaproteobacteria*) was the most abundant OTU across all samples and occurred in high concentrations in the more decomposed samples closer to shore. These data suggest the presence of a relationship between the occurrence of this genus and the decomposition state of the scum, and this relationship is supported by other studies which have observed an increase in *Aeromonas* during bloom decline (Shi et al. 2011, Cai et al. 2014). A possible interaction between *Aeromonas* and *Microcystis* is supported by studies showing that *Aeromonas* exhibits chemotaxis to other *Cyanobacteria* such as *Aphanizomenon flos-aquae* (Kangatharalingam et al. 1991). The nature of this interaction, however, remains elusive, as both positive and negative interactions between these genera have been reported. A symbiotic interaction is supported by the observation that microcystin extracted from *Microcystis* enabled a previously non-culturable *Aeromonas* to be isolated and grown (Pan et al. 2008). In contrast, *Aeromonas* has been shown to display algicidal activity against *Microcystis aeruginosa* (Chen et al. 2012, Kang et al. 2012, Liu et al. 2012). Berg et al. (2009) observed that isolated strains of *Caulobacter* and *Brevundimonas* (both belonging to *Caulobacteraceae* within *Alphaproteobacteria*) enhanced *Dolichospermum* and *Microcystis* growth. These genera have rarely been described in studies investigating bacterial communities in cyanobacterial phycospheres (Eiler & Bertilsson 2004, Berg et al. 2009), but were among the second and third most abundant OTUs in our samples, suggesting their functions in the cyanobacterial phycosphere need further investigation. Other taxa among the top 25 accounted for <5% and included taxa which have previously been associated with *Microcystis* blooms, such as *Flavobacterium*, *Pseudomonas* and *Sphingomonas* (Shia et al. 2010, Cai et al. 2014). Previous studies have found these genera were present in initial *Microcystis wesenbergii* colonies but disappeared with disaggregation of these colonies (Wang et al. 2015). *Sphingomonas* and *Flavobacterium* are also bacterial genera that are known to degrade cyanobacterial toxins and other organic complex compounds (Valeria et al. 2006, Berg et al. 2009, Dziallas & Grossart 2011). Their presence, particularly in sites that had high microcystin concentrations and were dominated by *Microcystis* colonies, supports their proposed association with maintaining colonies and toxin degradation. Further experimental studies would be required to confirm this suggestion.

Shifts in microcystin concentrations and quotas

Results from the Sanger sequencing of the *Cyanobacteria* samples suggest that *Microcystis* is the only microcystin-producing species in our samples, a finding which is consistent with a recent survey of toxin-producing planktonic *Cyanobacteria* across New Zealand (Wood et al. 2017b). There was no apparent relationship between microcystin concentrations or microcystin cell quotas and bacterial community structure or dominant OTUs. As noted above, bacterial taxa previously associated with microcystin degradation were identified in the samples, and the lower concentrations of microcystin at these sites could be due to a longer exposure to these bacteria.

In general, microcystin quotas were similar to those reported for other *Microcystis* in other New Zealand lakes (Wood et al. 2011, 2012, Puddick et al. 2016). Reasons for notable differences in the quotas among samples are difficult to determine. The higher quotas at Sites 1 and 2 in Bay A fits with the suggestion that microcystins may provide a protective function for the cells, such as resistance to oxidative stress (Zilliges et al. 2011). In contrast, the microcystin quotas in Bay B were much higher at the outer edge of the scum, and this fits with other studies that have shown upregulation of microcystin production during periods of active bloom formation (Wood et al. 2011, 2012). The findings of the present study suggest that microcystin production is likely triggered by multiple variables, and could have numerous ecological functions (Harke et al. 2016).

CONCLUSIONS

The results of this study demonstrate that *Cyanobacteria* genera differ in their ability to withstand the harsh conditions (e.g. fluctuating DO and pH, exposure to high UV) they are exposed to in dense scums (Hypothesis 1). The ability to cope with the extreme conditions present in scums may partly explain the prevalence of *Microcystis* in cyanobacterial blooms worldwide. Analysis of non-cyanobacterial RNA-derived OTUs showed significant differences between bacterial communities in areas of the scum that were recently formed compared to those that

were breaking down (confirming Hypothesis 2). The composition of the bacterial communities was similar to those found in previous studies, with *Proteobacteria* being the most abundant phylum across all samples. We found no evidence to support our final hypothesis that bacterial community composition or the presence of certain heterotrophic bacteria influences microcystin quotas. The marked variability in microcystin quota among sites regardless of whether the scum was recently formed or breaking down suggests that multiple biotic and abiotic factors effect microcystin production and degradation in environmental samples.

Acknowledgements. This research was supported by the New Zealand Ministry of Business, Innovation and Employment (UOWX1503; Enhancing the health and resilience of New Zealand lakes), the Marsden Fund of the Royal Society of New Zealand (12-UOW-087; Toxic in crowds), the Royal Society of New Zealand International Research Staff Exchange Scheme Fellowship (MEAT Agreement 295223) and the Marie Curie International Research Staff Exchange Scheme Fellowship (PIRSES-GA-2011-295223). We thank Tara McAllister (Canterbury University) for field assistance, Marc Jary (Cawthron Institute) for fieldwork logistics support, Lisa Floerl (Cawthron) for assistance with Fig. 1A, and Ronald Ram (University of Waikato) for phosphorus analysis.

LITERATURE CITED

Amemiya Y, Kato K, Okino T, Nakayama O (1990) Changes in the chemical composition of carbohydrates and proteins in surface water during a bloom of *Microcystis* in Lake Suwa. Ecol Res 5:153–162

Anderson MJ (2001) A new method for non-parametric multivariate analysis of variance. Austral Ecol 26:32–46

APHA (American Public Health Association) (2005) Standard methods for the examination of water and wastewater. APHA, Washington, DC

Arii S, Tsuji K, Tomita K, Hasegawa M, Bober B, Harada KI (2015) Cyanobacterial blue color formation during lysis under natural conditions. Appl Environ Microbiol 81: 2667–2675

Bartram J, Carmichael WW, Chorus I, Jones G, Skulberg OM (1999) Eutrophication, cyanobacterial blooms and surface scums. In: Chorus I, Bartram J (eds) Toxic cyanobacteria in water: a guide to their public health consequences, monitoring and management. Spon Press, London, p 3–4

Beardall J, Stojkovic S, Larsen S (2009) Living in a high CO_2 world: impacts of global climate change on marine phytoplankton. Plant Ecol Divers 2:191–205

Benson D, Karsch-Mizrachi I, Lipman D, Ostell J, Wheeler D (2008) GenBank. Nucleic Acids Res 36:D25–D30

Berg KA, Lyra C, Sivonen K, Paulin L, Suomalainen S, Tuomi P, Rapala J (2009) High diversity of cultivable heterotrophic bacteria in association with cyanobacterial water blooms. ISME J 3:314–325

Bolch CJ, Blackburn SI (1996) Isolation and purification of Australian isolates of the toxic cyanobacterium *Microcystis aeruginosa* Kütz. J Appl Phycol 8:5–13

Brunberg AK (1999) Contribution of bacteria in the mucilage of *Microcystis* spp.(Cyanobacteria) to benthic and pelagic bacterial production in a hypereutrophic lake. FEMS Microbiol Ecol 29:13–22

Cai H, Jiang H, Krumholz LR, Yang Z (2014) Bacterial community composition of size-fractioned aggregates within the phycosphere of cyanobacterial blooms in a eutrophic freshwater lake. PLOS ONE 9:e102879

Caporaso JG, Kuczynski J, Stombaugh J, Bittinger K and others (2010) QIIME allows analysis of high-throughput community sequencing data. Nat Methods 7:335–336

Carey CC, Ibelings BW, Hoffmann EP, Hamilton DP, Brookes JD (2012) Eco-physiological adaptations that favour freshwater cyanobacteria in a changing climate. Water Res 46:1394–1407

Carmichael WW (2001) Health effects of toxin-producing cyanobacteria: 'the CyanoHABs'. Hum Ecol Risk Assess 7:1393–1407

Casamatta DA, Wickstrom C (2000) Sensitivity of two disjunct bacterioplankton communities to exudates from the cyanobacterium *Microcystis aeruginosa* Kützing. Microb Ecol 40:64–73

Chen H, Fu L, Luo L, Lu J, White WL, Hu Z (2012) Induction and resuscitation of the viable but nonculturable state in a cyanobacteria-lysing bacterium isolated from cyanobacterial bloom. Microb Ecol 63:64–73

Cole JR, Wang Q, Fish JA, Chai B and others (2014) Ribosomal Database Project: data and tools for high throughput rRNA analysis. Nucleic Acids Res 42:D633–D642

Cottrell MT, Kirchman DL (2000) Natural assemblages of marine proteobacteria and members of the Cytophaga-Flavobacter cluster consuming low-and high-molecular-weight dissolved organic matter. Appl Environ Microbiol 66:1692–1697

Dell'Anno A, Danovaro R (2005) Extracellular DNA plays a key role in deep-sea ecosystem functioning. Science 309: 2179

De Philippis R, Vincenzini M (1998) Exocellular polysaccharides from cyanobacteria and their possible applications. FEMS Microbiol Rev 22:151–175

Dziallas C, Grossart HP (2011) Temperature and biotic factors influence bacterial communities associated with the cyanobacterium *Microcystis* sp. Environ Microbiol 13:1632–1641

Edgar RC (2010) Search and clustering orders of magnitude faster than BLAST. Bioinformatics 26:2460–2461

Edgar RC, Flyvbjerg H (2015) Error filtering, pair assembly and error correction for next-generation sequencing reads. Bioinformatics 31:3476–3482

Edgar RC, Haas BJ, Clemente JC, Quince C, Knight R (2011) UCHIME improves sensitivity and speed of chimera detection. Bioinformatics 27:2194–2200

Eiler A, Bertilsson S (2004) Composition of freshwater bacterial communities associated with cyanobacterial blooms in four Swedish lakes. Environ Microbiol 6:1228–1243

Fallon R, Brock T (1979) Lytic organisms and photooxidative effects: influence on blue-green algae (cyanobacteria) in Lake Mendota, Wisconsin. Appl Environ Microbiol 38: 499–505

Flouri T, Ijaz U, Mahé F, Nichols B, Quince C, Rognes T (2015) VSEARCH GitHub repository. Release 1.0. 16; 2015. Database: GitHub, https://github.com/torognes/vsearch

Funari E, Testai E (2008) Human health risk assessment

related to cyanotoxins exposure. Crit Rev Toxicol 38: 97–125

Harke MJ, Steffen MM, Gobler CJ, Otten TG, Wilhelm SW, Wood SA, Paerl HW (2016) A review of the global ecology, genomics, and biogeography of the toxic cyanobacterium, *Microcystis* spp. Harmful Algae 54:4–20

Havens KE (2008) Cyanobacteria blooms: effects on aquatic ecosystems. In: Hudnell HK (ed) Cyanobacterial harmful algal blooms: state of the science and research needs. Springer Science & Business Media, New York, NY, p 733–747

Hitzfeld BC, Höger SJ, Dietrich DR (2000) Cyanobacterial toxins: removal during drinking water treatment, and human risk assessment. Environ Health Perspect 108: 113–122

Ibelings BW, Maberly SC (1998) Photoinhibition and the availability of inorganic carbon restrict photosynthesis by surface blooms of cyanobacteria. Limnol Oceanogr 43:408–419

Jasti S, Sieracki ME, Poulton NJ, Giewat MW, Rooney-Varga JN (2005) Phylogenetic diversity and specificity of bacteria closely associated with *Alexandrium* spp. and other phytoplankton. Appl Environ Microbiol 71: 3483–3494

Kang YH, Park CS, Han MS (2012) *Pseudomonas aeruginosa* UCBPP-PA14 a useful bacterium capable of lysing *Microcystis aeruginosa* cells and degrading microcystins. J Appl Phycol 24:1517–1525

Kangatharalingam N, Wang L, Priscu JC (1991) Evidence for bacterial chemotaxis to cyanobacteria from a radioassay technique. Appl Environ Microbiol 57:2395–2398

Kolmonen E, Sivonen K, Rapala J, Haukka K (2004) Diversity of cyanobacteria and heterotrophic bacteria in cyanobacterial blooms in Lake Joutikas, Finland. Aquat Microb Ecol 36:201–211

Kouzminov A, Ruck J, Wood SA (2007) New Zealand risk management approach for toxic cyanobacteria in drinking water. Aust N Z J Public Health 31:275–281

Langlet D, Geslin E, Baal C, Metzger E and others (2013) Foraminiferal survival after long-term *in situ* experimentally induced anoxia. Biogeosciences 10:7463–7480

Liu YM, Wang MH, Jia RB, Li L (2012) Removal of cyanobacteria by an *Aeromonas* sp. Desalination Water Treat 47:205–210

Louati I, Pascault N, Debroas D, Bernard C, Humbert JF, Leloup J (2015) Structural diversity of bacterial communities associated with bloom-forming freshwater cyanobacteria differs according to the cyanobacterial genus. PLOS ONE 10:e0140614

Manage PM, Kawabata Z, Nakano S (2000) Algicidal effect of the bacterium *Alcaligenes denitrificans* on *Microcystis* spp. Aquat Microb Ecol 22:111–117

Mengoni A, Tatti E, Decorosi F, Viti C, Bazzicalupo M, Giovannetti L (2005) Comparison of 16S rRNA and 16S rDNA T-RFLP approaches to study bacterial communities in soil microcosms treated with chromate as perturbing agent. Microb Ecol 50:375–384

Oksanen J, Blanchet FG, Kindt R, Legendre P and others (2013) Package 'vegan'. Community ecology package, version 2. https://cran.r-project.org/web/packages/vegan/index.html

Oliver RL, Hamilton DP, Brookes JD, Ganf GG (2012) Physiology, blooms and prediction of planktonic cyanobacteria. In: Whitton BA (ed) Ecology of cyanobacteria II. Springer, Heidelberg, p 155–194

Paerl HW (1988) Nuisance phytoplankton blooms in coastal, estuarine, and inland waters. Limnol Oceanogr 33: 823–843

Paerl HW, Huisman J (2009) Climate change: a catalyst for global expansion of harmful cyanobacterial blooms. Environ Microbiol Rep 1:27–37

Paerl HW, Otten TG (2013) Harmful cyanobacterial blooms: causes, consequences, and controls. Microb Ecol 65: 995–1010

Paerl HW, Fulton RS, Moisander PH, Dyble J (2001) Harmful freshwater algal blooms, with an emphasis on cyanobacteria. Sci World J 1:76–113

Pan G, Hu Z, Lei A, Li S (2008) Effect of crude microcystin on the viable but non-culturable state of *Aeromonas sobria* in aquatic environment. Hupo Kexue 20:105–109

Parveen B, Ravet V, Djediat C, Mary I, Quiblier C, Debroas D, Humbert JF (2013) Bacterial communities associated with *Microcystis* colonies differ from free-living communities living in the same ecosystem. Environ Microbiol Rep 5:716–724

Paul VJ (2008) Global warming and cyanobacterial harmful algal blooms. In: Hudnell HK (ed) Cyanobacterial harmful algal blooms: state of the science and research needs. Springer Science & Business Media, New York, NY, p 239–257

Pereira S, Zille A, Micheletti E, Moradas-Ferreira P, De Philippis R, Tamagnini P (2009) Complexity of cyanobacterial exopolysaccharides: composition, structures, inducing factors and putative genes involved in their biosynthesis and assembly. FEMS Microbiol Rev 33: 917–941

Perrie A, Milne JR (2012) Lake water quality and ecology in the Wellington Region: states and trends. Rep No. 1927217059. Greater Wellington Regional Council, Wellington

Pollard PC, Young LM (2010) Lake viruses lyse cyanobacteria, *Cylindrospermopsis raciborskii*, enhances filamentous-host dispersal in Australia. Acta Oecol 36: 114–119

Pruesse E, Quast C, Knittel K, Fuchs BM, Ludwig W, Peplies J, Glöckner FO (2007) SILVA: a comprehensive online resource for quality checked and aligned ribosomal RNA sequence data compatible with ARB. Nucleic Acids Res 35:7188–7196

Puddick J, Wood SA, Hawes I, Hamilton DP (2016) Fine-scale cryogenic sampling of planktonic microbial communities: application to toxic cyanobacterial blooms. Limnol Oceanogr Methods 14:600–609

Rashidan K, Bird D (2001) Role of predatory bacteria in the termination of a cyanobacterial bloom. Microb Ecol 41: 97–105

Robarts RD, Waiser MJ, Arts MT, Evans MS (2005) Seasonal and diel changes of dissolved oxygen in a hypertrophic prairie lake. Lakes Reservoirs: Res Manag 10:167–177

Salomon PS, Janson S, Granéli E (2003) Molecular identification of bacteria associated with filaments of *Nodularia spumigena* and their effect on the cyanobacterial growth. Harmful Algae 2:261–272

Shen H, Niu Y, Xie P, Tao M, Yang X (2011) Morphological and physiological changes in *Microcystis aeruginosa* as a result of interactions with heterotrophic bacteria. Freshw Biol 56:1065–1080

Shi L, Cai Y, Kong F, Yu Y (2011) Changes in abundance and community structure of bacteria associated with buoyant *Microcystis* colonies during the decline of cyanobacterial

bloom (autumn–winter transition). Ann Limnol-Int J Limnol 47:355–362

Shia L, Cai Y, Wang X, Li P, Yu Y, Kong F (2010) Community structure of bacteria associated with *Microcystis* colonies from cyanobacterial blooms. J Freshw Ecol 25:193–203

Shunyu S, Yongding L, Yinwu S, Genbao L, Dunhai L (2006) Lysis of *Aphanizomenon flos-aquae* (Cyanobacterium) by a bacterium *Bacillus cereus.* Biol Control 39:345–351

Spungin D, Pfreundt U, Berthelot H, Bonnet S and others (2016) Mechanisms of *Trichodesmium* demise within the New Caledonian lagoon during the VAHINE mesocosm experiment. Biogeosciences 13:4187–4203

Stewart I, Seawright A, Shaw G (2008) Cyanobacterial poisoning in livestock, wild mammals and birds — an overview. In: Hudnell HK (ed) Cyanobacterial harmful algal blooms: state of the science and research needs. Springer Science & Business Media, New York, NY, p 613–637

Turner AM, Chislock MF (2010) Blinded by the stink: nutrient enrichment impairs the perception of predation risk by freshwater snails. Ecol Appl 20:2089–2095

Valeria AM, Ricardo EJ, Stephan P, Alberto WD (2006) Degradation of microcystin-RR by *Sphingomonas* sp. CBA4 isolated from San Roque reservoir (Córdoba–Argentina). Biodegradation 17:447–455

Wang Q, Garrity GM, Tiedje JM, Cole JR (2007) Naive Bayesian classifier for rapid assignment of rRNA sequences into the new bacterial taxonomy. Appl Environ Microbiol 73:5261–5267

Wang W, Zhang Y, Shen H, Xie P, Yu J (2015) Changes in the bacterial community and extracellular compounds associated with the disaggregation of *Microcystis* colonies. Biochem Syst Ecol 61:62–66

Whitton BA (2012) Ecology of cyanobacteria II: their diversity in space and time. Springer, Heidelberg

Wood SA, Rueckert A, Hamilton DP, Cary SC, Dietrich DR (2011) Switching toxin production on and off: intermittent microcystin synthesis in a *Microcystis* bloom. Environ Microbiol Rep 3:118–124

Wood SA, Dietrich DR, Cary SC, Hamilton DP (2012) Increasing *Microcystis* cell density enhances microcystin synthesis: a mesocosm study. Inland Waters 2:17–22

Wood SA, Borges H, Puddick J, Biessy L and others (2017a) Contrasting cyanobacterial communities and microcystin concentrations in summers with extreme weather events: insights into potential effects of climate change. Hydrobiologia 785:71–89

Wood SA, Maier MY, Puddick J, Pochon X, Zaiko A, Dietrich DR, Hamilton DP (2017b) Trophic state and geographic gradients influence planktonic cyanobacterial diversity and distribution in New Zealand lakes. FEMS Microbiol Ecol 93:fiw234

Worm J, Søndergaard M (1998) Dynamics of heterotrophic bacteria attached to *Microcystis* spp. (Cyanobacteria). Aquat Microb Ecol 14:19–28

Wu X, Kong F, Zhang M (2011) Photoinhibition of colonial and unicellular *Microcystis* cells in a summer bloom in Lake Taihu. Limnology 12:55–61

Zilliges Y, Kehr JC, Meissner S, Ishida K and others (2011) The cyanobacterial hepatotoxin microcystin binds to proteins and increases the fitness of *Microcystis* under oxidative stress conditions. PLOS ONE 6:e17615

Editorial responsibility: Ilana Berman-Frank, Ramat Gan, Israel

Submitted: April 20, 2017; Accepted: August 29, 2017
Proofs received from author(s): November 21, 2017